

Evaluating Perceptual fidelity of Text to 3D Models

Anonymous CVPR submission

Paper ID *****

Abstract

The field of text-to-3D generative methods has seen remarkable progress in recent times, driven by a series of breakthroughs. Despite this progress, the existing evaluation metrics often focus on a single criterion, such as the alignment between the input text and the generated 3D models, but they do not comprehensively evaluate the quality of the generated 3D model itself. Traditional methods for evaluating 3D models typically measure the distance between generated and reference shape distributions. However, these methods are not readily applicable to text-conditioned generative tasks due to the difficulty in obtaining a comprehensive reference set, given the vast range of natural language inputs. In this work, we propose a novel approach to evaluate the visual perception of generated 3D models using surface normal and visual feature analysis. Surface normals provide crucial information about the geometry of a surface, describing aspects such as surface orientation, curvature, and shape. Visual features provide a comprehensive understanding of the image's content and context.

020 †

1. Introduction

022 Based on the recent traction in the area of Text-to-3D
 023 models, there have also been many methods introduced
 024 to evaluate the generated 3D models based on the input
 025 query. These evaluation methods check against the fidelity
 026 of 3D model based on the text input GPT-4V(ision)[11],
 027 T3Bench[3]. To evaluate the geometric consistency of the
 028 generated 3D models, we use surface normal analysis as
 029 a key metric. First, we generate 3D models from text in-
 030 puts using a state-of-the-art text-to-3D model, represented
 031 as triangular meshes. Surface normals are then computed
 032 directly from the mesh geometry, serving as ground truth
 033 for comparison. To analyze the models from different
 034 perspectives, we capture 2D images from both canonical
 035 (e.g., front, side) and non-canonical (e.g., oblique, tilted)
 036 viewing angles. For surface normal prediction, we utilize
 037 StableNormal[12], a robust model designed to predict sur-

038 face normals from images under complex lighting and geo-
 039 metric conditions. The predicted normals from StableNor-
 040 mal are compared with the mesh-derived normals using cos-
 041 sine difference as the primary metric, which measures the
 042 angular discrepancy between the two sets of normals. To
 043 ensure that only valid regions of the model are evaluated,
 044 a masking procedure is applied to exclude irrelevant pix-
 045 els from the background. This approach allows us to as-
 046 sess the geometric fidelity of the 3D models across multiple
 047 views and varying levels of complexity, providing insight
 048 into the performance of text-to-3D generative models. We
 049 have also taken inspiration from text-to-Image evalua-
 050 tion methods [5], text-to-3DModel evaluation methods [7], [2].

2. Methodology

051 Our proposed methodology evaluates the fidelity of 3D sur-
 052 face reconstruction by combining quantitative metrics with
 053 qualitative visualizations. The framework begins with mesh
 054 preprocessing, where vertex and face data are extracted, fol-
 055 lowed by the projection of image-based features onto the
 056 mesh. Normal maps generated by the model are compared
 057 with ground truth using multiple evaluation metrics. Cosine
 058 similarity is computed for pixel-wise normal vector align-
 059 ment, capturing directional differences, while the struc-
 060 tural similarity index (SSIM) quantifies perceptual simili-
 061 arities. Additionally, learned perceptual image patch simi-
 062 larity (LPIPS)[13] is employed to measure perceptual fidelity us-
 063 ing pre-trained neural networks such as AlexNet and VGG.
 064 We also consider using a more recent method[4] to com-
 065 pute FID score used specifically for Image generation. To
 066 enhance evaluation reliability, masked regions are incorpo-
 067 rated, focusing computations only on valid, unoccluded ar-
 068 eas of the normal maps. The variance of surface features,
 069 such as mean, standard deviation, and variance, is quan-
 070 tified and visualized on the 3D mesh using Open3D, pro-
 071 viding insights into spatial feature distribution. Heatmaps
 072 visualize cosine similarity and SSIM metrics, while sta-
 073 tistical summaries, including variance statistics, are gen-
 074 erated. The implementation integrates Python libraries like
 075 PyTorch, Scikit-image, and Matplotlib for metric computa-
 076 tions and visualizations, ensuring an efficient pipeline for
 077

078 comprehensive evaluation. This multi-faceted approach en-
 079 ables a robust analysis of reconstructed surfaces, blending
 080 traditional image-level metrics with 3D geometric insights
 081 to support meaningful comparisons and advancements in
 082 3D reconstruction techniques. While new Gaussian Splat-
 083 ting methods like LGM[9], DreamBeast[6], we evaluate the
 084 3D models generated by ProlificDreamer[10]. We eval-
 085 uate the prompt "A 3D model of an adorable cottage with a
 086 thatched roof"

087 2.1. Texture Feature point Analysis

088 **Texture Feature Point Analysis** Texture feature point anal-
 089 ysis is a key part of evaluating the spatial distribution and
 090 consistency of features across the reconstructed 3D surface.
 091 This analysis focuses on projecting image-based DINO-
 092 V2[8] features onto the mesh and quantifying their variance,
 093 standard deviation, and mean to capture feature stability and
 094 alignment. The process enables a deeper understanding of
 095 the texture fidelity in the reconstructed model, highlighting
 096 areas where feature representations may vary significantly
 097 across different views or reconstructions.

098 **Feature Projection and Mapping** Feature extraction
 099 begins by identifying and projecting relevant texture points
 100 from input images onto the corresponding 3D mesh ver-
 101 tices. These features, derived from image patches, are
 102 mapped to the closest vertices using a KD-tree-based near-
 103 est neighbor search, which efficiently matches 2D image
 104 locations to 3D surface points. Each vertex is then assigned
 105 a feature vector, allowing a consistent texture representation
 106 across the surface.

107 **Variance and Consistency Quantification** For each
 108 feature point on the mesh, the variance, standard deviation,
 109 and mean of feature values across different views are com-
 110 puted. These metrics are used to assess the consistency of
 111 the features, indicating the stability and reliability of texture
 112 information for each vertex. High variance suggest areas
 113 where feature points lack stability, potentially due to occlu-
 114 sions or inconsistent texture mapping across images, while
 115 lower variance reflects a stable and uniform feature repre-
 116 sentation.

117 **Visualization of Feature Variance** To provide a spatial
 118 understanding of feature consistency, variance values are vi-
 119 sualized directly on the 3D mesh. Each vertex is colored
 120 based on its variance, creating a visual map of texture sta-
 121 bility across the surface. High-variance regions are high-
 122 lighted to indicate areas with potential instability in texture
 123 representation, while low-variance regions show where tex-
 124 ture mapping is consistent and reliable. This visualization
 125 is saved as a 3D .obj file, allowing easy inspection. Figure
 126 of variance is shown in image 3

127 **Interpretation and Use** Texture feature point analysis
 128 offers insights into the spatial consistency of textures on
 129 3D surfaces, highlighting potential areas of improvement

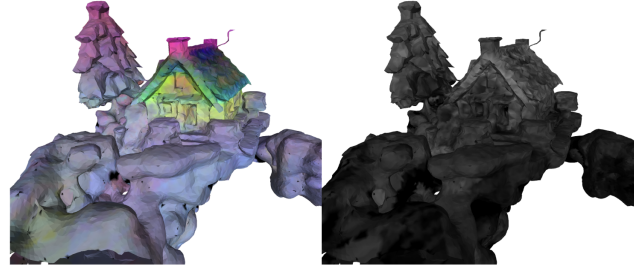


Figure 1. Left: shows the mean DINO-v2 features, Right: shows the standard deviation of the features.

in texture mapping and feature alignment. By integrating variance visualization and statistical reporting, this analysis serves as a robust tool for evaluating texture fidelity, enabling model developers to refine their approaches and enhance the visual realism of reconstructed surfaces.

130 2.2. Surface Normal Analysis

131 To evaluate the geometric consistency of the generated 3D
 132 models, we use surface normal analysis as a key metric.
 133 First, we generate 3D models from text inputs using a
 134 state-of-the-art text-to-3D model, represented as triangular
 135 meshes. Surface normals are then computed directly from
 136 the mesh geometry, serving as ground truth for comparison.
 137 To analyze the models from different perspectives, we cap-
 138 ture 2D images from both canonical (e.g., front, side) and
 139 non-canonical (e.g., oblique, tilted) viewing angles. For sur-
 140 face normal prediction, we utilize StableNormal[12], a ro-
 141 bust model designed to predict surface normals from images
 142 under complex lighting and geometric conditions. The pre-
 143 dicted normals from StableNormal are compared with the
 144 mesh-derived normals using cosine difference as the pri-
 145 mary metric, which measures the angular discrepancy be-
 146 tween the two sets of normals. To ensure that only valid
 147 regions of the model are evaluated, a masking procedure is
 148 applied to exclude irrelevant pixels from the background.
 149 This approach allows us to assess the geometric fidelity of
 150 the 3D models across multiple views and varying levels of
 151 complexity, providing insight into the performance of text-
 152 to-3D generative models. We also considered to process the
 153 normal maps into 3D object inspired form [1].

154 The analysis of surface normals is a critical component
 155 of the proposed methodology, aiming to assess the accu-
 156 racy and perceptual fidelity of reconstructed 3D surfaces.
 157 This process evaluates the alignment and similarity of nor-
 158 mal maps generated by the reconstruction model against
 159 ground-truth normal maps using three complementary ap-
 160 proaches: cosine similarity, structural similarity (SSIM),
 161 and learned perceptual image patch similarity (LPIPS).

162 **Cosine Similarity** Cosine similarity is employed to
 163 measure the directional alignment of surface normals on a

169 per-pixel basis. Normal maps are first normalized to unit
 170 vectors, ensuring consistent magnitude across all normal
 171 vectors. The cosine similarity is then computed as the dot
 172 product of corresponding vectors, providing a scalar value
 173 between -1 and 1, where 1 indicates perfect alignment. The
 174 methodology further aggregates these values to compute av-
 175 erage, variance, and median cosine similarity scores, en-
 176 abling quantitative comparisons of directional accuracy.

177 **Structural Similarity (SSIM)** SSIM is used to eval-
 178 uate the perceptual similarity between the reconstructed and
 179 ground-truth normal maps. By comparing luminance, con-
 180 trast, and structural information, SSIM captures differences
 181 that are more aligned with human visual perception. This
 182 metric is computed pixel-wise across the entire normal map
 183 and visualized as a difference heatmap, highlighting areas
 184 with significant deviations.

185 Learned Perceptual Image Patch Similarity (LPIPS)
 186 LPIPS evaluates the perceptual quality of reconstructed nor-
 187 mals using deep learning-based feature representations. By
 188 leveraging pre-trained networks such as AlexNet and VGG,
 189 LPIPS captures high-level perceptual differences that go be-
 190 yond simple pixel-wise comparisons. The normal maps are
 191 resized and normalized to ensure compatibility with the net-
 192 work, and the LPIPS distance is computed for each pair of
 193 normal maps.

194 **Mask Integration** To ensure the robustness of the anal-
 195 ysis, a mask is applied to exclude invalid or occluded re-
 196 gions of the normal maps. This focuses the evaluation on
 197 relevant areas, preventing noisy or undefined regions from
 198 skewing the results.

199 **Visualization and Outputs** The results of surface nor-
 200 mal analysis are visualized through heatmaps that represent
 201 cosine similarity and SSIM metrics. These heatmaps pro-
 202 vide an intuitive understanding of normal alignment and
 203 perceptual fidelity across the surface. Additionally, statisti-
 204 cal metrics, including the mean and variance of cosine sim-
 205 ilarity and SSIM, are summarized in CSV files for quantita-
 206 tive comparison. The visualization of discrepancy in texture
 207 is shown in 2

208 This comprehensive analysis of surface normals enables
 209 a detailed assessment of reconstruction accuracy, combin-
 210 ing traditional geometric alignment metrics with advanced
 211 perceptual measures. The integration of visualization and
 212 statistical reporting further facilitates a deeper under-
 213 standing of model performance and areas for improvement.

214 3. Results

215 3.1. Surface Normal Analysis

216 Our results on evaluating 20 3D models generated by 5
 217 generative models, including the most recent work Prolif-
 218 ic-dreamer, plot shown in Figure 4, show that canonical views
 219 (Rear and Side_Left), demonstrated high geometric con-

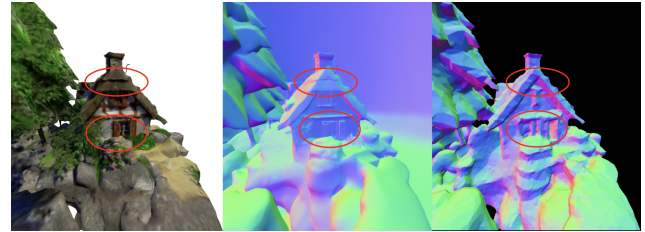


Figure 2. Shows mismatch in normals of the geometry and the texture. Left: Generated 3D model. Middle: 3D model’s normal. Right: Normals generated using StableNormals using the Left image.

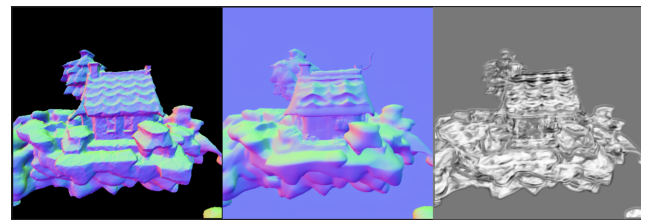


Figure 3. Left: Generated 3D model. Middle: 3D model’s normal. Right: SSIM of the Normals image

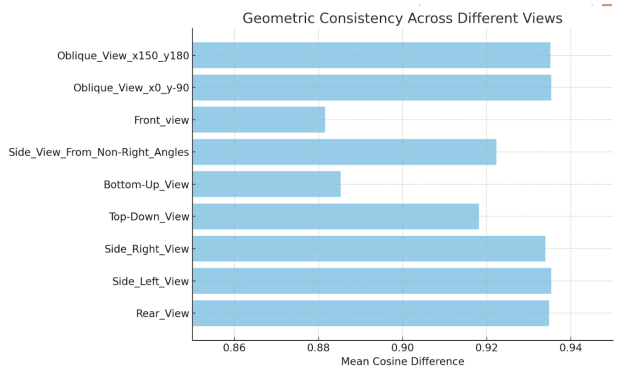


Figure 4. Plot of mean cosine differences of Surface Normal Analysis of 20 models, across various camera views.

220 consistency, with the highest mean cosine difference reaching
 221 0.93, indicating strong alignment between the predicted and
 222 ground truth surface normals. In contrast, non-canonical
 223 views (Side View from Non-Right Angles, Bottom-Up, and
 224 Top-Down), showed comparatively lower consistency, with
 225 the lowest mean cosine difference being 0.88. Although
 226 these non-canonical views also displayed relatively good
 227 consistency, these findings emphasize the importance of fo-
 228 cusing on non-canonical views to enhance the overall geo-
 229 metric fidelity of text-to-3D generative models.

230 References

- [1] Xu Cao and Takafumi Taketomi. Supernormal: Neural sur-
 231 face reconstruction via multi-view normal integration. In
 232

- 233 *Proceedings of the IEEE/CVF Conference on Computer Vi-*
 234 *sion and Pattern Recognition*, pages 20581–20590, 2024. [2](#)
- 235 [2] Yuze He, Yushi Bai, Matthieu Lin, Wang Zhao, Yubin Hu,
 236 Jenny Sheng, Ran Yi, Juanzi Li, and Yong-Jin Liu. T³
 237 bench: Benchmarking current progress in text-to-3d gener-
 238 ation. *arXiv preprint arXiv:2310.02977*, 2023. [1](#)
- 239 [3] Yuze He, Yushi Bai, Matthieu Lin, Wang Zhao, Yubin
 240 Hu, Jenny Sheng, Ran Yi, Juanzi Li, and Yong-Jin Liu.
 241 T³bench: Benchmarking current progress in text-to-3d gen-
 242 eration, 2024. [1](#)
- 243 [4] Sadeep Jayasumana, Srikumar Ramalingam, Andreas Veit,
 244 Daniel Glasner, Ayan Chakrabarti, and Sanjiv Kumar. Re-
 245 thinking fid: Towards a better evaluation metric for image
 246 generation, 2024. [1](#)
- 247 [5] Tony Lee, Michihiro Yasunaga, Chenlin Meng, Yifan Mai,
 248 Joon Sung Park, Agrim Gupta, Yunzhi Zhang, Deepak
 249 Narayanan, Hannah Teufel, Marco Bellagente, et al. Holis-
 250 tic evaluation of text-to-image models. *Advances in Neural*
 251 *Information Processing Systems*, 36, 2024. [1](#)
- 252 [6] Runjia Li, Junlin Han, Luke Melas-Kyriazi, Chunyi Sun,
 253 Zhaochong An, Zhongrui Gui, Shuyang Sun, Philip Torr, and
 254 Tomas Jakab. Dreambeast: Distilling 3d fantastical animals
 255 with part-aware knowledge transfer, 2024. [2](#)
- 256 [7] Zhiqiu Lin, Deepak Pathak, Baiqi Li, Jiayao Li, Xide Xia,
 257 Graham Neubig, Pengchuan Zhang, and Deva Ramanan.
 258 Evaluating text-to-visual generation with image-to-text gen-
 259 eration. In *European Conference on Computer Vision*, pages
 260 366–384. Springer, 2025. [1](#)
- 261 [8] Maxime Oquab, Timothée Darcet, Théo Moutakanni, Huy
 262 Vo, Marc Szafraniec, Vasil Khalidov, Pierre Fernandez,
 263 Daniel Haziza, Francisco Massa, Alaaeldin El-Nouby, Mah-
 264 moud Assran, Nicolas Ballas, Wojciech Galuba, Russell
 265 Howes, Po-Yao Huang, Shang-Wen Li, Ishan Misra, Michael
 266 Rabbat, Vasu Sharma, Gabriel Synnaeve, Hu Xu, Hervé Je-
 267 gou, Julien Mairal, Patrick Labatut, Armand Joulin, and Piotr
 268 Bojanowski. Dinov2: Learning robust visual features with-
 269 out supervision, 2024. [2](#)
- 270 [9] Jiaxiang Tang, Zhaoxi Chen, Xiaokang Chen, Tengfei Wang,
 271 Gang Zeng, and Ziwei Liu. Lgm: Large multi-view gaussian
 272 model for high-resolution 3d content creation, 2024. [2](#)
- 273 [10] Zhengyi Wang, Cheng Lu, Yikai Wang, Fan Bao, Chongxuan
 274 Li, Hang Su, and Jun Zhu. Prolificdreamer: High-fidelity and
 275 diverse text-to-3d generation with variational score distilla-
 276 tion, 2023. [2](#)
- 277 [11] Tong Wu, Guandao Yang, Zhibing Li, Kai Zhang, Ziwei Liu,
 278 Leonidas Guibas, Dahua Lin, and Gordon Wetzstein. Gpt-
 279 4v(ision) is a human-aligned evaluator for text-to-3d genera-
 280 tion, 2024. [1](#)
- 281 [12] Chongjie Ye, Lingteng Qiu, Xiaodong Gu, Qi Zuo,
 282 Yushuang Wu, Zilong Dong, Liefeng Bo, Yuliang Xiu, and
 283 Xiaoguang Han. Stablenormal: Reducing diffusion variance
 284 for stable and sharp normal. *ACM Transactions on Graphics*
 285 (*TOG*), 2024. [1](#), [2](#)
- 286 [13] Richard Zhang, Phillip Isola, Alexei A Efros, Eli Shechtman,
 287 and Oliver Wang. The unreasonable effectiveness of deep
 288 features as a perceptual metric. In *CVPR*, 2018. [1](#)